 doi:10.20944/preprints201905.0152.v1

Contribution to the understanding of "stick-slip" friction and creep-groan phenomena in automotive brake materials.

Peter Filip* and Seong K. Rhee**

*SIU Carbondale, Center for Advanced Friction Studies, Carbondale, IL 62901
**SKR Consulting, LLC, Northville, MI48167

Abstract

This contribution addresses dry sliding friction of a "Non-Asbestos Organic" friction material (pad) rubbed against a pearlitic grey cast iron disc. This configuration is commonly used in brakes in US, Europe and Asia. The initial stage of friction is of particular interest when addressing "creep-groan" phenomena occurring in passenger and sport utility vehicles with automatic transmissions. The custom built Universal Friction Tester allowing the variation of sliding speed, test temperature, normal load, stiffness and humidity of the system was used in this experiment in combination with surface analysis by polarized light microscopy, scanning electron microscopy and stylus profilometry. The obtained results indicate that the "stick" phase in the so-called "stick-slip" phenomenon does not really exist. The surfaces of pad and disc are in continuous relative movement. The complexity of surfaces does not allow for a definitive description of exact mechanisms responsible for the detected changes of friction forces. The observed friction process can be rather described as a stretching with possible localized relaxations causing the jerky behavior in the stretching phase, followed by slip between two materials in contact. Understanding of factors contributing to the stretching at different scale levels of friction system is necessary for development of proper models. An accurate friction model should also incorporate the vibrational element introduced by phenomena occurring at the friction surfaces. The absence of heterogeneous regions on the friction surface and "evenly distributed friction level" can help when mitigating creep-groan in the investigated brake system. Understanding of factors on different scales of friction is also required when developing the improved brakes.

Introduction

When a vehicle is about to move slowly from a complete stop, or when a vehicle comes to a stop from a relatively slow speed, the sliding interface/brake system can generate vibrations with a frequency between 1 and 30 Hz. This vibration is transmitted through the frame and suspension leading to the short (typically within 0.3 s) resonant vibration of the panels in the passenger compartment of a vehicle. The typically observed frequency of this short resonant vibration ranges between 150 and 550 Hz and the entire phenomenon is called creep-groan. The mechanism of the low frequency vibration generated in brake is poorly understood. It is often explained by the so-called "stick-slip" phenomenon. The "stick-slip" was addressed extensively at different levels. Numerous studies refer to a long historical background [1]. The "friction laws" initially described by DaVinci (16th century),

 doi:10.20944/preprints201905.0152.v1

Amontons (1699), and Coulomb (1781) remained purely empirical until Bowden and Tabor proposed the "microscopic interpretation" of friction, based on the observation that only a tiny part of the contact area, the so called effective area, is engaged in the friction process. They argued that the micro-contacts (interlocking asperities) representing this tiny area have to deform plastically and the stress always exceeds the yield point. Based on this work, friction only depends on the mechanical characteristics of the material and the elasto-plastic properties are the key feature of dry friction [5]. The "static friction coefficient" also depends on the (stick) time prior to the onset of sliding due to slow plastic relaxation of the stressed micro-contacts, which leads to an increase of the effective contact area. However, the situation is usually more complicated, for instance, in the brake friction materials where the generated wear debris forms a complex friction layer between two rubbing surfaces [6]. This friction layer can be continuous or "patchy" and depending on its structure and chemistry, it can completely separate the bulk materials (pad and disc) with their initial asperities. In these circumstances, the additional phenomena can play a relevant role.

In general, the friction in brakes (and elsewhere) arises on at least three different scales. The most intimate contact usually happens on the mentioned i) friction layer, which can be only few nanometers and typically few micrometers thick and can serve as the first level "force transmitting medium." Friction layer typically consists of partially or fully sintered small particulates (ranging from few nanometers to micrometers) and contains solid lubricants and abrasives [7, 8]. Depending on the capacity of this friction layer "to separate" the contact of solids (pad and disc), and on its ability to fully accommodate the shear stresses, the ii) deformation, fracture, further transport processes and phase transformations in volume adjacent to the pad and disc surfaces and typically up to 20 micrometers underneath the friction layer occur. Finally, the iii) bulk material and the entire system can represent the "zone" where dynamics of the containment have impact on the friction [9]. It was demonstrated that the "stick-slip" phenomenon also depends on these "system parameters" including the inertia, stiffness and mass of the moving parts.

There are several models addressing the "stick-slip" friction that include the effects of molecular/asperity size, previous history, sliding velocity, various relaxation effects/times and system parameters. They all are based on different mechanical or molecular properties of the surfaces of interacting friction couples [7]. The most widely discussed models of "stick-slip" involve the i) surface topography model, the ii) the velocity dependent model, and the iii) distance dependent model.

In the ***surface topology model***, the "stick-slip" is explained in terms of roughness of sliding surfaces [11]. Topography related "stick-slip" is due to "climbing" followed by a rapid sliding "down" of the slider. As the slider climbs the asperity, a resisting force increases in this "stick" stage. Once the slider reaches the peak, it will move rapidly down to the valley and this results in a quick slip. The phenomenon can be regular if the surface corrugations are regular or irregular which is more typical for the randomly rough surfaces. Topography dependent "stick-slip" is usually observed

Preprints (www.preprints.org) | NOT PEER-REVIEWED | Posted: 13 May 2019 doi:10.20944/preprints201905.0152.v1

in the sliding of macroscopically rough surfaces, and, as often demonstrated after development of the surface force apparatus (SFA) and the atomic and lateral force microscopy (AFM/LFM), also on the molecular/atomic level [11, 12, 13]. The periodicity of the AFM tip slipping over the "clean surface without wear" observed in LFM experiments correlates somehow with the atomic/molecular relief topography of the same surface observed in normal AFM mode. But the positions of the maxima and minima of lateral and normal forces are slightly shifted relative to each other. The controlling factors of topography related stick-slip friction are the surface roughness, and the elastic and inertial properties of the sliding surfaces. A stiffer material will have shorter slip phase because of shorter recoil to the elastic equilibrium. Plastic deformation of the asperities is reduced with increased hardness and the friction pattern approaches the contour trace of the surfaces. Both experiments and model calculations revealed that in order to be able to observe the stick-slip in AFM experiments, it is necessary to use a combination of a soft cantilever and a strongly interacting (stiff) surfaces. The softer is the contact the more energy dissipates and stick-slip can be completely eliminated [12].

The ***velocity dependent models*** of "stick-slip" friction apply usually to the contacts with films between the rubbing materials. A high static friction results from the film solidification when friction materials are not moving relatively to each other. Once the shearing force exceeds the value corresponding to static friction force, the film melts and lubricates which results in a lower kinetic friction force. "Stick-slip" occurs as the film goes through successive freezing-melting stages. At the critical velocity, at which the melting of layer occurs, is calculated from solution of equations of motion [14].

The distance dependent "stick-slip" friction models involve a characteristic distance and also time required for two asperities to increase their adhesion strength after coming into contact. This model requires that the rough macroscopic surfaces adhere through their microscopic asperities of characteristic length D_c. During friction process, each surface must first creep the distance D_c at a relatively high friction force, and, after breaking the adhered contact, continue to slide at a lower friction force. The reason for the decrease of the friction force is that the new asperity contact, which forms as rapidly as the old ones break, will have only very short time for adhesion. In the creep regime, the surfaces slowly accelerate at the beginning of slip and rapidly decelerate to a stop at the end of the slip. The friction force remains high during the creep stage of the slip but once the surfaces have moved the characteristic distance D_c, the static friction rapidly drops to the kinetic value. It is obvious that there exists a relationship between the creep distance D_c, sliding velocity, and effective time of contact (time = D_c/sliding velocity). Any system for which the static friction is higher than the kinetic friction will exhibit "stick-slip" friction for certain values of stiffness K, mass m and sliding velocities V. Baumberger et al. [15] showed that the paper on paper system exhibited a critical velocity V_c, which scaled differently with the stiffness K in the "creep regime" ($V_c \sim e^{-CK/m}$) and in the "inertia-dominated regime" ($V_c \sim K^{-2}$). The (creep) distance dependent model is often used to describe dry friction in metal on metal and rock on

 doi:10.20944/preprints201905.0152.v1

rock sliding but it can apply also to molecularly smooth surfaces with surfactants when friction force usually increases with the time of contact [10].

None of the friction/"stick-slip" models developed is generally applicable to all friction scenarios. The models usually fit or work for particular real systems. This further supports the general observation that the friction and wear are system properties and neither results nor trends obtained for one system should be applicable to another. It is also obvious, that due to the complexity of tribology phenomena, the friction models lack the necessary sophistication and they typically do not involve the phenomena occurring on different scales mentioned above and described in more detail in [9].

Experienced brake engineers are aware of the fact that the creep groan phenomenon occurs prior to the breakaway (static) friction. In other words, it appears that micro-vibration is taking place prior to the macro-vibration commonly known as "stick-slip".

The authors will discuss the detected observations in relation to the above described friction models, and try to elucidate physical mechanisms involved in the micro-vibration stage.

Experimental

The friction tests were performed at two sliding velocities 0.01 mm/s and 0.001 mm/s, respectively, the applied normal load (dead weight) was 84 N, relative humidity was 42 %, and testing temperature (of slider) was 150^{o}C (commonly called "hot creep" in brake industry). The samples were brought into contact with the preheated cast iron slider and remained in the "zero" position at full normal load (84 N) for 60 s before the test start. Parallel alignment between the tested pad sample and the cast iron slider was achieved by adjusting a sphere in the sample holder/head.

The Universal Friction Tester (UFT) used in this study was developed at the Center for Advanced Friction Studies, Southern Illinois University Carbondale [16]. Figure 1 shows the schematic of the friction tester (a) and the precise 4-quadrant laser sensor (b) allowing for measuring the position/displacement of the "stationary" sample holder head with the accuracy of +/- 1 nm. It is assumed that this measured displacement is equal to the displacement of the "stationary" brake pad sample, rigidly fixed to the sample holder head. A NMB hybrid stepper motor performing 256 micro-steps per 1.8^{o} rotation controlled the movement of the cast iron slider. The rotational movement of the motor was controlled by Centent microstepping drive with sinusoidal signal.

Preprints (www.preprints.org) | NOT PEER-REVIEWED | Posted: 13 May 2019 doi:10.20944/preprints201905.0152.v1

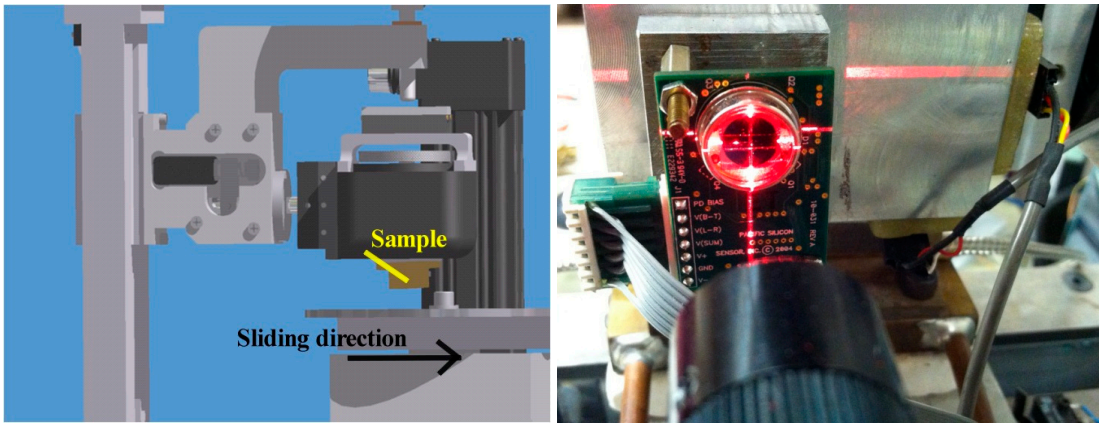

a) b)

Figure 1. CAD drawing of the testing head showing the (stationary) sample holder and the (moving) slider (a) and the 4-quadrant laser sensor allowing a precise determination of sample holder position (accuracy +/- 1 nm).

The stepper motor is linked with a worm gear having a ground fine threaded lead screw that drives the slider with a very large torque and stiffness. The system was programmed to initially move the cast iron slider towards the load cell, which was followed by an "away movement" in the opposite direction in order to "zero-out" the load cell. A calibrated precision load cell using an adjustable spring force mechanism measures the friction force. The National Instruments data acquisition system (DAQ) with the maximum acquisition rate capacity of 250 000 samples per second was employed and the "convenient" sampling rate of 25 000 samples/s was used in this experiment.

The tested pad samples with dimensions 12.7 mm x 12.7 mm x 5 mm were cut off the so-called Non-Asbestos Organic OE production brake pads, burnished in accord with the SAE J2430 procedure. The pearlitic grey cast iron slider was manufactured out of an OE production brake disc. The chemical composition of the disc is: 3.05 wt. % C, 1.7 wt. % Si, 0.9 wt. % Mn, 0.1 wt. % S, 0.2 wt. % P. The brake pad is a phenolic resin matrix composite material containing 15 different polymeric, ceramic and metallic materials. Before testing, the surface of the slider was prepared using 400 grit SiC paper.

Surfaces of the tested samples were inspected using the Scanning electron microscopy (FEI, model Quanta FEG 450) and stylus profilometry (Mahr profilometer with 2µm diamond tip).

Results and Discussion

Figure 2 shows typical dependences of the friction force variation with displacement of the cast iron slider and time elapsed from the initiation of the friction test for two applied sliding velocities 0.01 mm/s (red) and 0.001 mm/s (black).

Preprints (www.preprints.org) | NOT PEER-REVIEWED | Posted: 13 May 2019 doi:10.20944/preprints201905.0152.v1

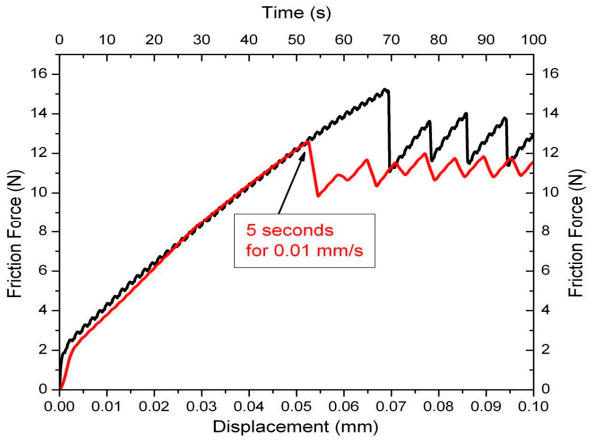

Figure 2. Typically measured dependences of friction force vs. slider displacement for two different sliding velocities. "Stick-slip" phenomena are quite different. Red dependence is for 0.01 mm/s and black dependence is for 0.001 mm/s. Sampling rate: 25 000 samples/s.

There are five obvious distinctions detected for these two testing velocities. The initial breakaway force characterizing the static friction is considerably larger for the slower sliding velocity (1 μm/s), the entire "stretch" phase prior to the first breakaway is jerky for the slower velocity and smooth for the higher sliding velocity (10 μm/s), the "slip" phase is much faster for the slower test and takes ~5 s after the initial break-away of the faster test, and there are differences in the initial stiffness when dependences obtained for slower and faster tests, respectively, are compared.

Figure 3 shows typical surface topology of the investigated pad (a) and rotor (b) samples as measured on 10 mm x 10 mm areas. This rectangular area represents almost the entire pad sample surface and a randomly selected region within the "friction trace" marked on the cast iron slider. Both pad sample and cast iron slider show characteristic grooving in the direction of sliding.

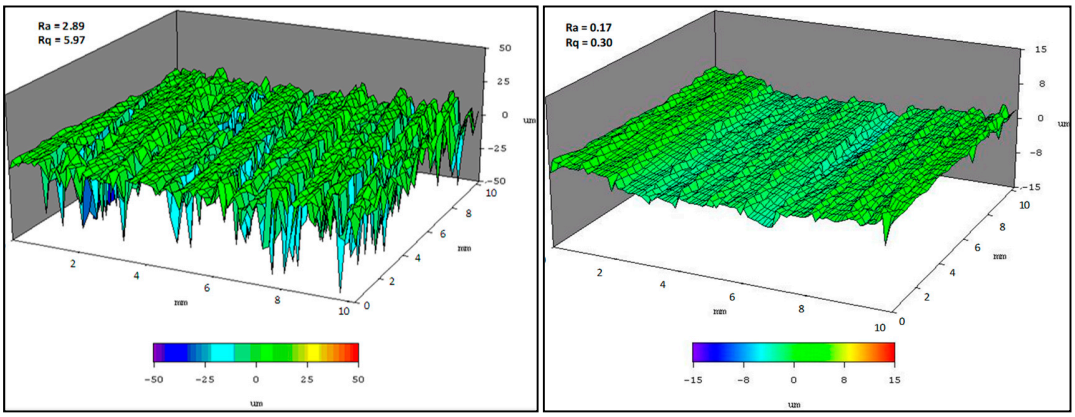

a) b)

Figure 3. Surface topography of pad (a) and cast iron slider sample (b).

Preprints (www.preprints.org) | NOT PEER-REVIEWED | Posted: 13 May 2019 doi:10.20944/preprints201905.0152.v1

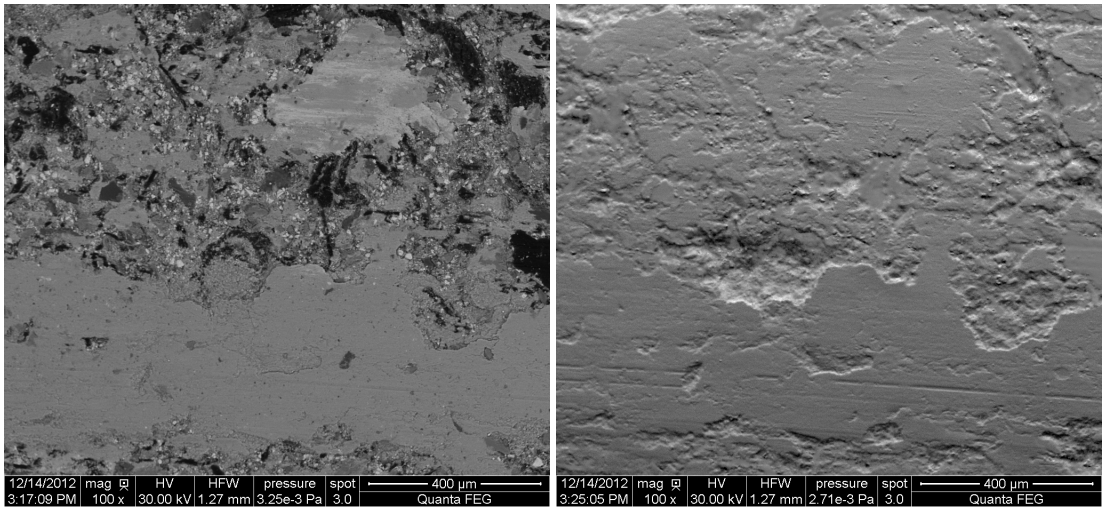

a) b)

Figure 4. Back scattered SEM image of typical pad surface (a) and the corresponding topography (b) image.

The pad material has a rougher surface than slider cast iron, which is related to differences in their microstructures.

The heterogeneous microstructure of the pad material is shown in the back-scattered electron image given in Fig. 4a. The ceramic abrasive particles responsible for grooving of pad and disc surfaces are easily seen along with “patchy” friction layer developed well on the majority of the surface shown in the image, which can be also seen from the corresponding SEM topography image given in Fig. 4b. When inspecting Fig. 4a, it is obvious from the backscattered electron image that the different areas of the pad friction surface exhibit different chemistry. Without performing the exact chemical analysis of the surface, it is well known that the brighter regions are formed by heavier elements with a higher atomic number and the darker areas are formed by the lighter elements. The topography image (Fig. 4b) shows that the friction contact occurs on the friction layer. It is possible to expect that the friction level will differ in the different parts of the surface shown in Fig. 4, since the “layer forming materials” with different chemistry will have different properties. For instance the elasto-plastic properties of the asperities in brighter and darker regions, respectively, will differ, the capacity to create adhesive junctions with the rubbing counter-face will differ, the viscosity of the friction layer and its capacity to melt/freeze will differ, critical speeds for “stick-slip” friction will differ, load transfer to the sub-layer regions will be different, and one can continue with the list of differences. The different regions will therefore very probably exhibit different break-away forces and the measured dependences shown in Fig. 2 represent “a collective” response from numerous different events. It can be expected that certain elements of all three above-discussed “stick-slip friction models” and possibly their combinations can be applied simultaneously to this complex friction process.

 doi:10.20944/preprints201905.0152.v1

The same friction force-cast iron slider displacement dependence obtained at the lower sliding velocity of 1 μm/s, as shown in Fig. 2, is given again in Fig. 5. In addition to the force-displacement information (black line), Fig. 5a also shows the instantaneous "in plane" displacement of the pad sample (blue line), as measured by the 4-quadrant detector. Figure 5b also shows the corresponding "in-plane" sliding velocity of the pad sample (blue line). It is termed "in-plane" displacement and velocity, respectively, since the 4-quadrant sensor also detects the "out of plane" movements. The plane is considered to be sliding plane, parallel with the pad sample and slider surface. The bold blue arrows in Figs. 5 a and b show the direction "away from the load cell," displacements "towards the load cell" are in the opposite direction. The black arrows in Fig. 5b indicate the difference in force oscillation amplitude, which will be discussed later.

When the cast iron slider is about to start its movement at the beginning of test (position "zero" for force and slider displacement at the horizontal axis of Figs. 5a and b), the pad sample was displaced by almost 6 μm in direction toward the load cell. This displacement is related to initial procedure of "force zeroing" as described in the experimental. It is easily seen in Fig. 5a that the pad sample, being dragged by the cast iron slider, starts to move away from the load cell after the test starts. Nevertheless, there is an oscillatory movement of the pad superimposed on the general motion. This displacement ("stretch") away from the load cell is happening in three distinct intervals marked by slope of the pad displacement versus testing time dependence. The first interval between approximately *i)* 0 to 5 s of testing time, corresponds to the displacement of about 1 μm (from ~ 6 μm to ~ 5 μm), followed by *ii)* ~ 5 to ~ 20 s interval with the pad sample displacement of ~3 μm (from ~ 5 μm to ~ 2 μm), and the third interval *iii)* between ~ 20 s and ~ 70 s, in which the pad sample moves additional ~ 0.5 μm away from the load cell in direction of the cast iron slider motion. In the first time interval (0 to ~ 5 s), the slope is "less steep" when compared to the slope observed in the second interval (~ 5 to ~ 20 s) and the lowest slope was seen in the final interval (~ 20 to ~ 75 s) before the first break-away force (static friction force F_s) is reached. At this point, the pad sample moves distinctly (approximately 1.3 μm) in the opposite direction towards the load cell and against the continuous motion of the cast iron slider. This is typically called "slip" phase.

Preprints (www.preprints.org) | NOT PEER-REVIEWED | Posted: 13 May 2019 doi:10.20944/preprints201905.0152.v1

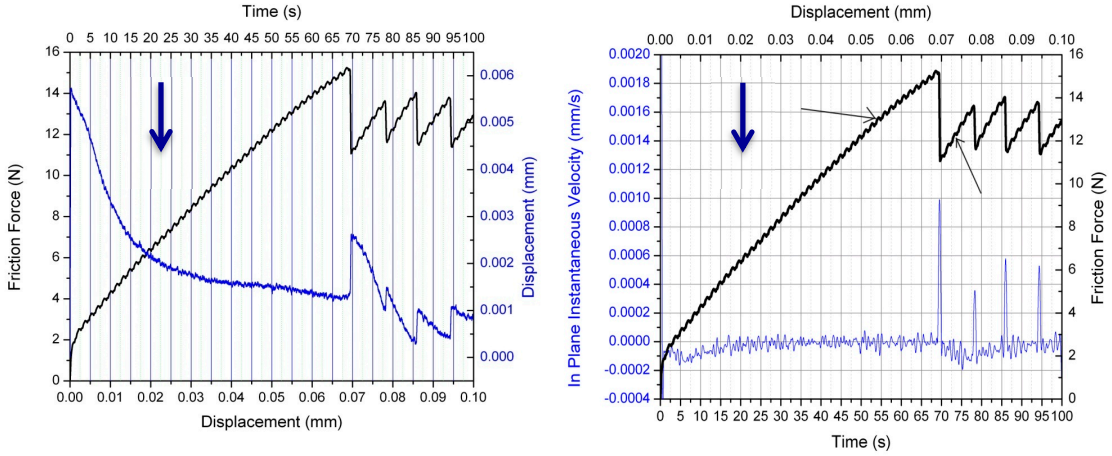

a) b)

Figure 5. Friction force (black) vs. slider displacements and pad sample displacement (blue) vs. slider displacement (a), and friction force (black) versus slider displacement, and in-plane instantaneous velocity of pad sample (blue) vs. slider displacement (b).

The initial trend in the force-pad displacement slope is somehow repeated after the first "slip" phase and then it changes towards a minimum slope in the consecutive "stick" events (blue dependence in Fig. 5a). As easily seen from Fig. 5a, the changes in the displacement direction of the pad sample well correlate with the so-called "stick-slip" phenomena detected for the force versus slider displacement (black line) dependence.

Similar close correlation was also observed for the in-plane instantaneous velocity of the pad sample as shown in Fig. 5b by the blue line. In the first ~ 20 s, the velocity of the sample is negative (away from load cell) and its general trend reflects the described slope changes. The velocity trend is becoming increasingly negative in the first ~ 5 s interval, then it changes to a "less negative" trend and reaches the "zero value" at ~ 20 s of testing. One has to appreciate, however, that in addition to the mentioned general velocity trend, the instantaneous velocity of pad sample changes rapidly and oscillates about the general trend curve. So in the ~20 to ~70 s time interval, the pad sample moves away from the load cell (Fig. 5a) with oscillating value of velocity smaller than approximately +/- 0.2 µm/s (Fig. 5b). Note that the cast iron slider does not stop its continuous movement at 1 µm/s. The pad sample would "interlock" or "stick" to the cast iron slider (no relative movement) only at conditions when their velocities would be equal (level and direction). At the instant when the pad sample and the slider reach a common velocity, it may be said that the two parts are moving together because of "interlocking" or "sticking". After the two parts reach a common velocity, the subsequent process can be described as stretching, with possible localized relaxations causing the jerky behavior. This process of micro "interlock-stretch-release" or "stick–stretch-slip" continues until the first macro-breakaway ("static friction") occurs (Fig. 5b). After the first macro-breakaway, this same micro process continues, which leads to the macro "interlock-

 doi:10.20944/preprints201905.0152.v1

stretch-release ("stick-stretch-slip") again. In other words, the micro "interlock-stretch-release" process precedes the macro "interlock-stretch-release process. So it may be said that the micro process is associated with one spring while the macro process with a different spring. For example, we may view the friction film as one spring and the pad or the pad-holder assembly as another spring. A careful examination of the long wiggly line of Figure 5 indicates that the line actually consists of two parts with two different slopes, ignoring the first interval of system adjustment, which suggests that there are at least two springs involved in the long stretch phase before the first macro-release (slip), and then another spring for the macro-slip. For the slow sliding speed of 0.001 mm/s, the small oscillations (the second and third intervals) show a frequency of roughly 0.6 Hz while the large oscillations after the macro-breakaway show a frequency of 0.13 Hz. Also the small oscillations following the first macro breakaway show 0.6 Hz again and the slope of the micro oscillations is similar to the average slope of the first and second intervals of the oscillations before the first breakaway, which suggests the same mechanisms before the first macro-breakaway is in operation here again. So, referring to Figure 5a, the pad sample assembly initially undergoes a rapid displacement (soft spring), followed by slower displacement (hard spring). Therefore, it can be said that the second interval is dominated by a soft spring and the third interval by a hard spring. When the second-spring force exceeds the frictional force, the macro breakaway occurs. Clearly the "dynamic friction" after the first major breakaway is lower than the breakaway friction ("static"). Referring back to Figure 2, as the sliding speed increases to 0.01 mm/s, the major breakaway friction is reduced (speed dependent) and also the subsequent "dynamic friction" is reduced (speed dependent), which is contrary to one of Amonton-Coulomb's laws of friction. The stretching measured and reported here occurred in the plane of contact but this does not need to be necessarily case in all friction situations. Understanding of the contribution to this stretching at different scale levels (friction layer, zone adjacent to the friction surface underneath the friction layer, and the bulk material/system) is also necessary when developing proper friction models.

The instantaneous in-plane acceleration of pad sample is shown in Fig. 6.

Preprints (www.preprints.org) | NOT PEER-REVIEWED | Posted: 13 May 2019 doi:10.20944/preprints201905.0152.v1

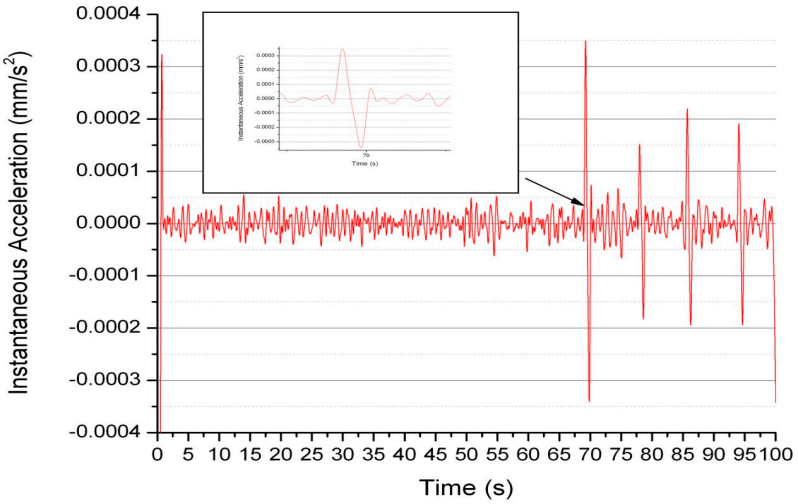

Figure 6. The instantaneous acceleration of pad sample plotted versus testing time. The insert highlights the single event marked by arrow.

Again, the sample acceleration direction changes in an oscillatory pattern and the observed "spikes" well correspond to the macro-breakaway friction phenomena. In spite of the fact that the acceleration of the pad sample reaches "zero value" when oscillating, the slider moves constantly and there is no real "stick" phase detected. In addition to the "spike" events detected at the breakaway moments, a comparatively large acceleration variation was seen during the initial stage of the movement. With the initiation of the cast iron slider movement, the force increases linearly and a high stiffness is typical for this period (Fig. 5). The not fully cured pad sample heated to 150°C contains organic materials, which soften and adhere well to the surface of the cast iron slider. This literally "glues" the pad sample to the cast iron slider during the 60 s initial period before the test starts. The pad/slider connection is broken after the force reaches approximately 1.35 N. A careful look at Figs. 5 and 6 also demonstrates that the sample is first moved/accelerates away from the loading cell and, when the adhesive contact is released, the pad sample moves rapidly towards the load cell. Similar phenomena can be observed in brakes when pads "freeze" to the cast iron discs or when a corrosive process joins them together. Obviously, these phenomena were not considered to be "stick-slip" friction and are commonly referred to as "stiction."

After reaching the strength of pad/slider junction (corresponding force of ~ 1.35 N), the increase of the cast iron slider displacement is accompanied with a less rigid "jerky" force-slider displacement pattern with a sub-linear trend. It should be noted that the "jerky pattern" was only detected when the sampling rate was high enough (in this case 25 000 samples/s). So the sampling capacity, in addition to the accurate measurement of the displacement, is very critical for proper friction measurements. Indeed, numerous researchers were not able to detect the "jerky pattern" during the stretching phase of the loading. Also, it is obvious that the faster testing eliminates the "jerking." One can speculate that the time is too short, so the attractive forces between the pad and slider cannot develop, which is in accord with all three above-

 doi:10.20944/preprints201905.0152.v1

described models. This experiment, however, is not able to provide a more detailed answer as what attractive forces are developing in the "stretching" phase before a rapid "slip" occurs. And it is not a surprise, since we do not have a good understanding of these interactions in considerably simpler systems studied by AFM or SFA [12, 13].

One can appreciate, however, that the amplitude and frequency of the "jerky" pattern changed after the first breakaway at approximately 70s of testing. The black arrows in Fig. 5b point to the different patterns. The amplitude of the force oscillation in the initial "stretching" phase is around 20 nm and reaches slightly more than 30 nm after the first breakaway in following "stretch" events. Obviously, the introduced vibration (see the acceleration changes in Fig. 6), related to the oscillatory changes detected, has an impact on the friction process and a different amplitude of "jerking" can result from this impact. An accurate friction model should also incorporate the vibrational element introduced by phenomena occurring at the friction surfaces. When looking at the nanometer size amplitudes, one can speculate that the phenomena occurring at the nano-level can be responsible for this oscillation. Again, however, the observed physical response of the force on slider displacement is obviously a result of collective actions in the tested system and a more complex and superimposed effects can be involved.

The force displacement is not showing a linear trend before the first breakaway force is reached. This indicates that not only elastic deformation occurs in this stage, which would be demonstrated by a classical "saw-tooth" behavior of the friction force. Kragelski [17] was one of the first scientists who suggested that the friction force does not need to be a linear rise prior the "slip." Holm suggested first that the irregularities in the "stretching" phase can be related to heterogeneities in the contact surfaces producing momentarily contact yielding prior the complete increase of the force to its maximum, and also to the slip portion of the process can disrupted by premature engagement of the rapidly slipping surface with the asperities on the opposing surface [6]. In his work, however, there was not a regularity of the jerky movement as detected in this research. Although we cannot fully disregards the philosophy applied in the models describing friction (listed above) or the suggestions made by Kragelski, Holm and others, it is easily seen from the performed analysis that the friction process is quite complex in these systems and a deeper understanding is required when developing models.

With respect to the creep-groan, observed in automobiles, it is possible to anticipate that the critical velocity will be achieved, since the stopping as well as the brake release and movement starting processes "happen" through a series of velocities. Obviously a faster release of the brake is advisable but the material change and a mitigation of the phenomena leading to a less oscillatory response in displacement of pad would be a possible solution. Obviously, the ideally "equal friction level" on the entire surface of pads and the absence of heterogeneities with different properties and friction levels (see Fig. 2a) would help when mitigating the creep groan phenomena in this type of brake design. A well developed, possibly

 doi:10.20944/preprints201905.0152.v1

homogeneous and stable friction layer can play an important role, however, the understanding of factors on different scales of friction is also required when developing the improved brakes.

In summary, if the pad sample and the sample holder were completely rigid, and if the sliding interface had zero friction, the sample and the sample holder would not vibrate while the cast iron slider moved. Since the pad sample and the sample holder were not rigid enough, and also due to the friction forces at the sliding interface, the pad sample/holder assembly is pulled in the direction of the cast iron slider initially. The pulling phase involves many micro "stick-stretch-slip" steps and this process continues until the assembly breaks away from the slider (macro breakaway; macro "stick-stretch-slip") in the opposite direction of the slider motion as the spring force of the sample assembly exceeds the friction force. It is believed that this overall process is taking place on a vehicle, the sample holder assembly corresponding to the caliper assembly and the slider to the disc. It appears that the micro "stick-stretch-slip" process leads to the creep groan phenomenon prior to the macro "stick-stretch-slip".

Conclusions

Not a real "stick" phase was observed during the so-called "stick-slip" friction experiment. The two counterparts – brake pad and cast iron slider - constantly move with respect to each other.

The observed friction process can be rather described as a stretching with possible localized relaxations causing the jerky behavior in the stretching phase, followed by slip between two materials in contact. This process can be described and understood in terms of "interlock-stretch-release" or "stick-stretch-slip". Two distinctive stages have been identified; micro "stick-stretch-slip" and macro "stick-stretch-slip".

Understanding of factors contributing to the stretching at different scale levels of friction system is necessary for development of proper models.

An accurate friction model should also incorporate the vibrational element introduced by phenomena occurring at the friction surfaces.

The absence of heterogeneous regions on the friction surface and "evenly distributed friction level" can help when mitigating creep-groan in the investigated brake system. Understanding of factors on different scales of friction is also required when developing the improved brakes.

References

[1] D. Dowson, History of Tribology, Longman, London (1979).
[2] H. J. Noh, H. Jang, Wear, Vol. 268, (2018) 400-401, 93-99.

[3] W. K. Lee, M. W. Shin, S. H Kim, H. Jang, M. H. Cho, Wear, Vol. 302, (2013), 1397-1403.
[4] T. H. Rhee, M. W. Shin, H. Jang, Tribology International, Vol. 94, (2016) 234-239.
[5] F. P. Bowden and D. Tabor, The Friction and Lubrication of Solids, Clarendon Press, Oxford (1950).
[6] P. Filip, Z. Weiss, D. Rafaja, On Friction Layer Formation in Polymer Matrix Composite Materials for Brake Applications, Wear. Vol. 252, (2002), 189-198.
[7] P. Filip: Friction and Wear of Polymer Matrix Composite Materials for Automotive Braking Industry, International Conference Braking 2002, Leeds UK, Professional Engineering Publishing, London, UK, 2002, 341 -354.
[8] J. Kukutschova, V. Roubicek, K. Malachova, Z. Pavlickova, R. Holusa, J. Kubackova, V. Micka, D. MacCrimmon, P. Filip: "Wear Mechanism in Automotive Brake Materials, Wear Debris and its Potential Environmental Impact," Wear Vol. 267, (2009), 807-817.
[9] P. J. Blau, Friction Science and Technology, Marcel Dekker, Inc. (1996).
[10] A. D. Berman, W. A. Ducker, J. N. Israelashvili, Experimental and Theoretical Investigations of Stick-Slip Friction Mechanisms, in B. N. J. Persson and E. Tosatti (eds.), Physics of Sliding Friction, Kluwer Academic Publishers, Dordrecht, Boston, London (1989), pp. 51 - 67.
[11] E. Rabinowicz, Friction and Wear of Materials, John Wiley and Sons, New York (1965).
[12] G. V. Dedkov, Nanotribology: Experimental Facts and Theoretical Models, Physics-Uspekhi, Vol. 43, No. 6, (2000), 541 – 572.
[13] Y. Mo, K. T. Turner, I. Szlufarska, Friction Laws at the Nanoscale, Nature, Letters, 457, (2009), 1116 – 1119.
[14] M. A. Thompson, M. O. Robbins, Origin of Stick-Slip Motion in Boundary Lubrication, Science, 250, (1990), 792-794.
[15] T. Baumberger, F. Heslot, B. Perrin, Crossover from Creep to Inertial Motion in Friction Dynamics, Nature, 367, (1994), 544 – 546.
[16] J. Boone, Design and Development of the Universal Friction Tester, M. Sc. Thesis, Southern Illinois University Carbondale.
[17] I. V. Kragelski, Friction and Wear, Butterworths, London, (1965).